SUPPLEMENTARY METHODS

Antibiotics. Bottromycin A_2 (BotA2) and bottromycin A_2 carboxylic acid (BotCA) standards were kindly provided by Prof. Rolf Müller and Dr. Joy Birkelbach, Helmholtz Institute for Pharmaceutical Research Saarland (HIPS), Helmholtz Centre for Infection Research (HZI), Saarbrücken, Germany. BotA2 and BotCA used in experiments were purified from culture broth of *Streptomyces* sp. VKM Ac-2945^T as described below. Both compounds were dissolved in 50% dimethyl sulfoxide (DMSO) aqueous solution to a final stock concentration of 20 mM. Mupirocin (Mup) was purchased from pharmacy. Erythromycin (Ery), chloramphenicol (Chl), levofloxacin (Lev), thiostrepton (Ths), borrelidin (Borr), cycloheximide (Chx), kanamycin (Kan), rifampicin (Rif), streptomycin (Str), kirromycin (Kirr) used as reference agents, were purchased from Sigma-Aldrich, Burlington, MA, USA. Tetracenomycin X (TcmX) was purified from culture broth of *Amycolatopsis* sp. A23 as described previously [1]. Microcin C (McC) was purified according to the published procedure [2].

Purification of BotA2 and BotCA. Preparative RP-HPLC was performed on a puriFlash® PF-4250 preparative chromatograph (Interchim, Montluçon, France) equipped with a VDSpher 100 C18-E (10 µm, 20×250 mm) column (VDS optilab, Berlin, Germany). UV-Vis detection was carried out at 205 and 254 nm. Eluent A consisted of 0.1% trifluoroacetic acid (TFA) (HPLC grade, Fisher Scientific, Loughborough, UK) in ultrapure water; eluent B was acetonitrile (HPLC gradient grade, Fisher Scientific, Loughborough, UK) containing 0.1% TFA. Ultrapure water was obtained using the HyperPureX purification system (Hyperpurex Instrument Technology, Shanghai, China). The flow rate was maintained at 20 mL/min. For BotCA, the gradient program was 0–25–28–33 min, 29–29–95–95% B, with a retention time of 24.5 min. For BotA2, the program was 0–15–25–30 min, 30–40–95–95% B, with a retention time of 19.3 min (Fig. S1).

The identity of the isolated compounds was first confirmed by analytical RP-HPLC using BotA2 and BotCA standards, and then by high-resolution mass spectroscopy (HRMS) analysis. Analytical RP-HPLC was carried out on an Agilent 1100 system (Agilent Technologies, Santa Clara, CA, USA) with a quaternary pump, equipped with an Ultisil XB-C18 (5 µm, 4.6×250 mm) column (Welch Materials, Shanghai, China) and a corresponding Ultisil XB-C18 (5 µm, 4.6×20 mm) guard column (Welch Materials, Shanghai, China). Eluent A was ultrapure water, eluent B was acetonitrile, and eluent C was 2% aqueous TFA. For BotA2, the analytical method applied was 0–10–12–14 min, 40–70–95–95% B, with a constant addition of 5% C, yielding a retention time of 6.9 min. For BotCA, the method was 0–30–31–34 min, 29–29–95–95% B, with a constant addition of 5% C, yielding a retention time of 22.6 min. The identity of the samples was further confirmed by HPLC-HRMS/MS analysis using the Orbitrap Exploris 240 mass spectrometer coupled with the Vanquish UHPLC system (Thermo Fisher Scientific, Waltham, MA, USA), equipped with a reversed-phase Acclaim™ 120 C18 (2.2 µm, 2.1×150 mm) column (Dionex, Sunnyvale, CA, USA). Eluent A was 0.1% formic acid in ultrapure water, eluent B was 0.1% formic acid in acetonitrile. Chromatographic separation was carried out at 45 °C in gradient elution mode at a flow rate of 0.4 mL/min. Gradient program was as follows: 0–3 min, 5% B; 3–17 min, 5–95% B; 17–21 min, 95% B; 21–22 min, 95–5% B. Injection volume was 10 µL and autosampler temperature was 4 °C. Mass spectra were acquired separately in both

positive and negative ionization modes. Heated electrospray ionization (ESI) source parameters were as follows: ion source voltage—3,500 V for positive ionization mode or 2,500 V for negative ionization mode; sheath/auxiliary/sweep gas—50/10/1 arb; ion transfer temperature—325 °C; vaporizer temperature—350 °C. Mass spectra were recorded with a full scan from 50 to 2,000 m/z. The resolution was 30,000 (for both MS^1 and MS^2 spectra), the RF lens—70%. MS^2 spectra were acquired in data-dependent acquisition (DDA) mode using dynamic exclusion-based precursor selection. Higher-energy collisional dissociation (HCD) fragmentation parameters were as follows: isolation window—1 m/z with isolation offset turned off; normalized collision energy—15%, 30%, 45%, and 60%; normalized automatic gain control (AGC) target—200% with a maximum injection time parameter set to “auto”.

Bacterial strains and cultivation conditions. The *Escherichia coli* BW25113 strain with a partial deletion of the *lptD* gene, codons 330 to 352 (referred to here as *E. coli lptD*^{mut}) was kindly provided by Dr. Alexander S. Mankin, University of Illinois, Chicago, IL, USA [3]. The *E. coli* JW5503-KanS strain carrying a deletion of the *tolC* gene (referred to here as *E. coli ΔtolC*) was obtained from the *E. coli* JW5503 strain by removing the kanamycin resistance cassette via Flp-assisted recombination [4]. *E. coli* JW5503 and *E. coli* BW25113 were kindly provided by Prof. Hironori Niki, National Institute of Genetics, Mishima, Shizuoka, Japan [5]. *E. coli ΔtolC* cells were transformed with pJC27 plasmids, encoding either a native or mutant *lacZ* gene [6]. The following mutations at the catalytic residue of β -galactosidase were used: Glu537Asp (GAA→GAC), Glu537Gly (GAA→GGA/GGG), corresponding to the plasmids pJC27-GAC, pJC27-GGA, and pJC27-GGG.

The *E. coli* SQ110 strain with the deletion of six rRNA operons (except for *rrnE*) and the *tolC* gene (referred to here as SQ110 ΔtolC) was kindly provided by Dr. Alexander S. Mankin [3]. Mutants resistant to Chl, Ery, or both of them were selected using the SQ110 ΔtolC strain, according to the procedure reported previously [1]. The *E. coli* SQ171 strain with the deletion of all seven rRNA operons and the *tolC* gene (referred to here as SQ171 ΔtolC), and transformed with the pCSacB (Kan^R) plasmid, which contains the wild-type *rrnB* operon, was kindly provided by Dr. Alexander S. Mankin [7, 8]. The pCSacB (Kan^R) plasmid was further replaced with the pLK35 (Amp^R) or pAM552 (Amp^R) plasmid encoding either the native (WT) or mutated *rrnB* operon, according to the procedure described previously [1].

Bacillus subtilis 168 was kindly provided by Stanislav S. Terekhov, Shemyakin-Ovchinnikov Institute of Bioorganic Chemistry, Moscow, Russia. *B. subtilis* 168 pHT01-cat and *B. subtilis* 168 pHT01-cfr were obtained as described previously [9].

Unless otherwise stated, all aforementioned bacterial strains were grown at 37 °C in Miller’s Lysogeny Broth (LB) medium supplemented with antibiotics, if required. *E. coli lptD*^{mut} and *E. coli ΔtolC* transformed with the pJC27 plasmids were cultivated in the presence of 10 μg/mL chloramphenicol. SQ110 ΔtolC strains were cultivated in the presence of 50 μg/mL kanamycin. SQ171 ΔtolC pLK35 and SQ171 ΔtolC pAM552 strains were cultivated in the presence of 100 μg/mL ampicillin. *B. subtilis* 168 pHT01-cat was cultivated in the presence of 5 μg/mL chloramphenicol. *B. subtilis* 168 pHT01-cfr was cultivated in the presence of 3 μg/mL chloramphenicol. Other bacterial strains were cultivated without antibiotics.

Agar diffusion assay on a panel of resistant mutants. Overnight cultures of SQ110 ΔtolC and SQ171 ΔtolC cells grown in the presence of relevant antibiotics were plated on 1.5% LB-agar solid medium supplied either with 50 μg/mL kanamycin or with 100 μg/mL ampicillin, respectively, and left to dry for a while until the next step. The following antibiotics were applied on the surface of agar plates coated with SQ110 ΔtolC or SQ171 ΔtolC cells: erythromycin (Ery, 5 mg/mL), levofloxacin (Lev, 25 μg/mL), tetracenomycin X (TcmX, 5 mg/mL), chloramphenicol (Chl, 2 mg/mL). In the center of each agar plate, a well was made and filled with 50 μL of 1 mM BotA2 dissolved in 30% acetonitrile aqueous solution. The plates were incubated overnight at 37 °C and scanned with the ChemiDoc™ Imaging System (Bio-Rad Laboratories, Hercules, CA, USA) using the "Cy5-blot" channel (emission filter 695 ± 50 nm). Images were analysed and visualized using the Image Lab™ software (version 6.0.1, Bio-Rad Laboratories, Hercules, CA, USA).

Determination of minimum inhibitory concentration (MIC). MIC values were determined using the standard liquid broth microdilution assay [10] in 96-well sterile plates and a total volume of 100 μL per well. Stock solutions of antibiotics were diluted 1:50 with 100 μL of fresh LB medium. Subsequently, 2-fold serial dilutions were performed and bacterial cells in the log growth phase diluted 1:100 with LB medium were added to each well. The plates were incubated overnight (16-20 h) at 37 °C with constant shaking at 200 rpm (Shaker-Incubator ES-20/80, BioSan, Riga, Latvia). Cell growth was assessed by scanning the OD_{600} with the VICTOR X5 Multilabel Plate Reader (PerkinElmer, Waltham, MA, USA).

***In vitro* translation in bacterial cell-free systems.** Firefly luciferase (Fluc) mRNA was prepared using the MEGAscript™ T7 Transcription Kit (Thermo Fisher Scientific, Waltham, MA, USA). Translation reactions (3 μL total volume) were carried out with the PURExpress® In vitro Protein Synthesis Kit (New England BioLabs, Ipswich, MA, USA) according to the manufacturer's protocol. Alternatively, the reactions (5 μL total volume) were carried out with *E. coli* S30 Extract System for Linear Templates (Promega, Madison, WI, USA) according to the manufacturer's instructions. Each reaction was supplied with 2 U of RiboLock RNase Inhibitor (Thermo Fisher Scientific, Waltham, MA, USA), 0.17 mM of D-luciferin sodium salt (Sigma-Aldrich, Burlington, MA, USA), 60 ng of Fluc mRNA, and aqueous solution of antibiotic or nuclease-free water instead. Stock antibiotic solutions were diluted with nuclease-free water to 10-fold final concentrations immediately before the experiment. Before the addition of mRNA, reaction tubes were pre-incubated at room temperature (RT) for 5 min and then placed back on ice. After the addition of mRNA, reaction mixtures were transferred into the 384-well white microplate. Chemiluminescence was continuously measured using the VICTOR X5 Multilabel Plate Reader (PerkinElmer, Waltham, MA, USA) at 37 °C for 1 h. The maximum Fluc accumulation rates were calculated (as an increment of light intensity units per second) and defined as the efficiency of translation reactions. The values were normalized to a positive control (nuclease-free water, assigned a value of 100%). The IC_{50} values of translation inhibition were calculated and visualized using the GraphPad Prism software (version 10.1.2, Dotmatics, Boston, MA, USA).

***In vitro* translation in a mammalian cell-free system.** The whole cell extract was prepared from the HEK293T cell line as described previously [11] with minor modifications: harvested cells were not

treated with lysolecithin buffer. Instead, they were immediately suspended in an equal volume of ice-cold hypotonic extraction buffer [20 mM HEPES-KOH (pH 7.5), 10 mM KOAc, 1 mM $Mg(OAc)_2$, 4 mM DTT and cOmplete™ EDTA-free Protease Inhibitor Cocktail (Roche, Basel, Switzerland)], incubated for 5 min on ice and disrupted in a tiny Dounce homogenizer by 20-25 strokes. The lysate was clarified by centrifugation for 10 min at 10,000 g at 4 °C. Aliquots were frozen in liquid nitrogen and stored at -80 °C.

Each translation reaction was carried out in a total volume of 10 µL and contained 5 µL of the HEK293T whole cell extract, translation buffer [20 mM HEPES-KOH (pH 7.5), 8 mM creatine phosphate, 1 mM DTT, 0.5 mM spermidine-HCl, 1 mM ATP, 0.2 mM GTP, 100 mM KOAc, 1 mM $Mg(OAc)_2$ and 25 µM of each amino acid], 2 U of Creatine Phosphokinase from rabbit muscle (Sigma-Aldrich, Burlington, MA, USA), 2 U of RiboLock RNase Inhibitor (Thermo Fisher Scientific, Waltham, MA, USA), 0.5 mM of D-luciferin sodium salt (Sigma-Aldrich, Burlington, MA, USA), 1 µL of either an antibiotic water solution or nuclease-free water as a positive control, and 100 ng of m^7G-capped and polyadenylated Fluc mRNA with the β-actin 5' UTR. The latter one was prepared using the mMESSAGE mMACHINE™ T7 Transcription Kit (Thermo Fisher Scientific, Waltham, MA, USA) and added as 1 µL water solution to the translation mixtures after they were pre-incubated for 5 min at 30 °C. Then, the mixtures were transferred into the pre-warmed 384-well white microplate, covered with a PCR plate seal and incubated in the CLARIOstar® Plus Microplate Reader (BMG Labtech, Ortenberg, Germany) at 30 °C with continuous measurement of the luciferase activity. The maximum Fluc accumulation rates were calculated and defined as the efficiency of translation reactions. The values were normalized to a positive control (assigned a value of 100%) and visualized using the GraphPad Prism software (version 10.1.2, Dotmatics, Boston, MA, USA).

Toe-printing assay. DNA templates (0.3 pmol) were expressed in a cell-free bacterial transcription-translation coupled system using the PURExpress® In Vitro Protein Synthesis Kit (New England BioLabs, Ipswich, MA, USA) in a total volume of 5 µL, following the manufacturer's protocol. All antibiotics were added to the final concentration of 50 µM. Negative control samples (indicated as "−") were supplemented with nuclease-free water instead of antibiotics. Before the addition of a DNA template, reaction mixtures were pre-incubated at RT for 5 min. Following the addition of a DNA template, the reactions were incubated at 37 °C for 20 min, then 1 pmol of the [^{32}P]-labeled NV1 or NV2 primer (Table S1) and 2 U of the AMV Reverse Transcriptase (Roche, Basel, Switzerland) were added, and reaction tubes were additionally incubated at 37 °C for 15 min. Reactions were terminated by the addition of 1 µL of 10 M NaOH followed by incubation at 37 °C for 15 min. The pH was further neutralized and stabilized by the addition of an equivalent amount of 10 N HCl, and then 200 µL of Resuspension Buffer [0.3 M NaOAc (pH 5.5), 5 mM EDTA, 0.5% SDS]. Thereafter, the samples were subjected to cDNA fragments purification using the QIAquick® PCR Purification Kit (Qiagen, Hilden, Germany) according to the manufacturer's protocol, instead of phenol-chloroform extraction. Resulting cDNA solutions were dried at 95 °C and dissolved in 10 µL of Formamide Loading Buffer [98% formamide, 10 mM EDTA (pH 8.0), 0.1% bromophenol blue, 0.1% xylene cyanol]. The sequencing reactions were performed using the USB® Thermo Sequenase Cycle Sequencing Kit (Affymetrix, Santa Clara, CA, USA) according to the manufacturer's protocol. The cDNA fragments, along with sequencing reactions, were resolved on a 6% polyacrylamide sequencing gel

containing 7 M urea in TBE buffer [90 mM Tris base, 90 mM boric acid, 2 mM EDTA, pH 8.3]. After electrophoresis, the gel was dried using the Savant™ Universal Vacuum System Plus with VaporNet® (UVS400A, Thermo Fisher Scientific, Waltham, MA, USA) at 80 °C for 1 h, and exposed to the phosphorimager screen overnight. The screen was scanned using the Typhoon™ FLA 9500 Biomolecular Imager (GE Healthcare, Chicago, IL, USA) or the FujiFilm Fluorescent Image Analyzer FLA-3000 (Fujifilm, Tokyo, Japan), and the images were processed using the Image Lab™ software (version 6.0.1, Bio-Rad Laboratories, Hercules, CA, USA).

Preparation of samples for Toe-seq analysis. A library of linear DNA templates was generated by PCR in the preceding work [12]. One template consisted of a T7 promoter, a 5' UTR (one of three types), an ORF containing a start codon, 30 randomized nucleotides, and 7 constant codons, followed by a 3' UTR (one of two types) and a barcode region. Next generation sequencing (NGS) of the library resulted in a dictionary representing each barcode matched up with its ORF sequence and both UTR sequences. The library of DNA templates was expressed in a bacterial transcription-translation coupled system using the PURExpress® In Vitro Protein Synthesis Kit (New England BioLabs, Ipswich, MA, USA) in the presence of 50 μM BotA2. Reactions supplied with nuclease-free water instead of BotA2 served as untreated controls. All reactions were prepared in two biological replicates. AMV Reverse Transcriptase (Roche, Basel, Switzerland) was further applied to synthesize cDNA fragments, which were further purified and elongated at their 3' end by 5 U of Terminal Transferase (New England BioLabs, Ipswich, MA, USA) supplied with 4 μM dATP. Poly(A)-tailed cDNA was then converted into dsDNA by Klenow Fragment (3'→5' exo-) (New England BioLabs, Ipswich, MA, USA) according to the manufacturer's protocol. After that, dsDNA fragments were additionally amplified with high-fidelity PCR. Purified PCR products were subjected to library preparation using the MGIEasy Universal DNA Library Prep Set (MGI Tech, Shenzhen, China) and sequenced on the MGIseq-2000 (MGI Tech, Shenzhen, China) at the Genomics Core Facility (ICBFM SB RAS, Novosibirsk, Russia).

Computational processing of Toe-seq data. Raw FastQ sequencing data were processed according to the reported procedure [12]. All the computations described below were performed using in-house Bash and Python scripts and the previously obtained dictionary. For each mRNA, read counts per nucleotide position were calculated as the number of reads ending at each position. Reads terminated at 5' UTR were summed and designated as FL values (the quantity of full-length cDNA fragments). Thereafter read counts per position were normalized to the total number of mapped reads and then multiplied by 10^6, resulting in the so-called counts per million (CPM). For each sense codon, normalized read counts associated with positions +16, +17, and +18 relative to the first nucleotide of the codon were summed up and divided by the total number of CPM of a given mRNA (CPM_{mRNA}). The resulting values reflect ribosome density distribution along the coding sequence and correspond to codons occupying the P-site of the ribosome. In addition, all CPM values associated with positions located between the start codon and the start codon +15 nucleotides were summed with the previously calculated FL values and divided by the corresponding CPM_{mRNA}. Next, we normalized the data of antibiotic-treated samples to that of control samples (nuclease-free water) by subtracting the corresponding ribosome densities. This step additionally

allows us to exclude non-specific reverse transcriptase products from further consideration. The resulting positive values represent the distribution of ribosome stalling probability (*StallProbability*) along the ORF sequence, whilst the negative values should be interpreted as truly “impossible” sites for antibiotic-specific ribosome stalling, not merely “zero probability”. The serial number of the codon associated with the maximum probability of ribosome stalling (*MaxStallProbability*) was defined as the main position of antibiotic-induced ribosome stalling (*StallPosition*) at a given mRNA. In the case of mRNAs containing a premature stop codon, only appropriate *StallProbability* values were considered to determine *MaxStallProbability* and *StallPosition*. All *StallProbability* values that fall outside the real range of ORF were excluded from the analysis in advance. Since the accuracy of the *MaxStallProbability* score depends on the mRNA coverage (designated here as CPM_{mRNA}), we introduced a *Likelihood* metric that takes into account the reliability of the calculated *MaxStallProbability* over the entire dataset. This metric was defined as follows:

$$Likelihood_i = MaxStallProbability_i \cdot 2^{lg\left(\frac{CPM_{mRNA,i} \cdot CPM_{mRNAc,i}}{\sum_j CPM_{mRNA,j} \cdot CPM_{mRNAc,j}}\right)}, \quad (1)$$

where $CPM_{mRNA,i}$ and $CPM_{mRNAc,i}$ stand for the total number of CPM attributed to a given mRNA (with the barcode = i) and obtained from antibiotic-treated and control samples, respectively. It is worth noting that we use *Likelihood* as a relative rather than an absolute metric. Likewise, we introduced another parameter named *cpmRNAratio*, which represents the similarity in mRNA coverage between two samples and is calculated as follows:

$$cpmRNAratio_i = \frac{CPM_{mRNA,i}}{CPM_{mRNAc,i}}, \quad (2)$$

The following criteria were further applied to extract the most relevant ribosome stalling sites from a dataset: (i) *MaxStallProbability* score should be higher than 0, (ii) *cpmRNAratio* should be within the interquartile range (IQR), (iii) mRNAs with CPM_{ORF}, CPM_{mRNAc}, and *Likelihood* values below the corresponding 25th percentile should be filtered out. Here, CPM_{ORF} is the number of CPM in mRNA coding region. The resulting datasets were used for further analysis.

Analysis of amino acid enrichment at the sites of BotA2-induced ribosome stalling. Both filtered datasets derived from BotA2-treated samples were used to extract ribosome stalling sites defined by the calculated *StallPositions*. The sequence of each site included amino acid residues corresponding to the codons occupying the E-, P-, and A-sites of arrested ribosomes. Sites associated with ribosome stalling at the start and stop codons, as well as at the second codon and codons 11-17, were excluded from the analysis to consider only variable region of mRNA. A total of 12,245 sites were applied as foreground sequences to the pLogo tool [13]. To generate background sequences, we extracted all possible 3-aa

motifs associated with codons at the 2nd, 3rd, and 4th positions of the ORF from the same entire mRNA libraries.

Analysis of codon enrichment at the sites of BotA2-induced ribosome stalling. Each filtered dataset derived from BotA2-treated samples was used to calculate relative occurrence of individual codons at E-, P-, and A-site positions among the identified stalling sites. Only sites associated with *StallPositions* 3-10 were included in the analysis, as they correspond to the variable region of mRNA. The obtained values were further normalized to codon frequencies (calculated from the same entire mRNA libraries) by subtraction, to account for possible codon bias. Therefore, the resulting negative values conform to underrepresented codons, while positive values indicate overrepresented ones.

LC-QTOF-MS analysis of samples prepared for GATRAL. LC-QTOF-MS analysis was performed using the Acquity UPLC System (Waters, Milford, MA, USA) coupled to a quadrupole time-of-flight (QTOF) mass spectrometer maXis Impact II (Bruker Daltonics, Bremen, Germany), equipped with an electrospray ionization (ESI) source. The sample (10 µL) was completely dissolved in 20 µL of deionized water. Then, 10 µL solutions were injected into the LC-QTOF-MS system. Chromatographic separation was carried out at 40 °C using a binary gradient at a flow rate of 0.2 mL/min on an Acquity UPLC BEH C18 (1.7 µm, 2.1×100 mm) column (Waters, Milford, MA, USA) coupled with Acquity UPLC BEH C18 VanGuard (1.7 µm 2.1×5 mm) pre-column (Waters, Milford, MA, USA). The mobile phase consisted of 5 mM (NH_4)OAc (pH 5.2) in water (solvent A), and 5 mM (NH_4)OAc (pH 5.2) in 90% acetonitrile (MeCN) (solvent B). Stepwise linear gradient: 0-3 min with 2% MeCN, 3-28 min from 2% to 40% MeCN, 28-30 min from 40% to 80% MeCN, 30-35 min with 80% MeCN, 35-37 min from 80% to 2% MeCN, 37-40 min with 2% MeCN. The mass spectrometer was operated in positive ionization mode. Total ion chromatograms (TICs) were acquired using the following settings: nebulizer pressure of 1.8 bar, drying gas flow rate of 5 L/min, and drying gas temperature of 180 °C. Mass spectrometer was calibrated daily using the external calibration standard ES Tuning Mix (Agilent Technologies, Santa Clara, CA, USA). Mass spectra were analyzed using the Compass DataAnalysis software (version 4.3, Bruker Daltonics, Bremen, Germany).

Agar diffusion assay using misreading error reporter systems. *E. coli ΔtolC* cells transformed with the pJC27 reporter systems were used as described previously [14]. In brief, the overnight culture of *E. coli ΔtolC* pJC27 was diluted 1:8 in 4 mL of warm (50 °C) 0.6% LB-agar supplemented with 10 µg/mL chloramphenicol. After a brief mixing, the cell suspension was poured on top of a 1.5% LB-agar plate (9 cm Petri dish) supplemented with 10 µg/mL chloramphenicol, and 80 µg/ml X-Gal (5-bromo-4-chloro-3-indolyl β-D-galactopyranoside). After the soft agar had solidified, antibiotics were applied on the surface of agar plates containing a reporter strain. The plates were incubated overnight at 37 °C and photographed on camera. The following stocks of antibiotics used were: kanamycin (Kan, 5 mg/mL), rifampicin (Rif, 10 mg/mL), streptomycin (Str, 5 mg/mL), bottromycin A_2 carboxylic acid (BotCA, 20 mM), bottromycin A_2 (BotA2, 20 mM), and bottromycin A_2 (indicated as (●), 500 µM).

Purification of $tRNA^{Gly}$. Total *E. coli* tRNA was aminoacylated with 0.5 mM glycine at 37 °C for 30 min using 5% S100 extract. Aminoacyl-tRNA was supplemented with two-fold excess of EF-Tu·GTP to form a ternary complex (aa-tRNA·EF-Tu·GTP) at 37 °C for 5 min. Ternary complex was purified on 1 mL

column Protino® Ni-IDA (Macherey-Nagel, Düren, Germany) according to the manufacturer's guidance. The eluted ternary complex was dissociated by addition of potassium acetate (pH 5.0) to a final concentration of 0.2 M, and aminoacyl-tRNA was phenol-extracted and precipitated with ethanol. The tRNA pellet was dissolved in ddH_2O and stored at -80 °C.

Preparation of initiation and ternary complexes. For a typical reaction of initiation complex formation, 1 μM 70S ribosomes were incubated with 5 μM mRNA, 2 μM fMet-$tRNA^{fMet}$ or 1.5 μM BODIPY-Met-$tRNA^{fMet}$,1.5 μM of IF1, IF2 and IF3 in the $TAKM_7$ buffer supplemented with 1 mM GTP and 2 mM DTT at 37 °C for 1 h. Ternary complexes of aa-tRNA·EF-Tu·GTP were prepared by pre-incubation of EF-Tu with 1 mM GTP, 3 mM phosphoenolpyruvate, 2 mM DTT,1% pyruvate kinase in the $TAKM_7$ buffer at 37 °C for 15 min, followed by addition of aa-tRNA and incubation for 5 min.

Preparation of uncharged tRNA. Total tRNA was isolated from *E. coli* BW25113 culture using the Total RNA and Small RNA Isolation Kit (Biolabmix, Novosibirsk, Russia), according to the manufacturer's protocol. Then, the purified tRNA was treated with 1U of RNase-free DNase I (1 U/μL) (Thermo Fisher Scientific, Waltham, MA, USA) in reaction buffer containing 40 mM Tris-HCl (pH 8.0), and 6 mM $MgCl_2$. Reactions were incubated at 37 °C for 1 h. After extraction with phenol saturated with 0.1 M citrate buffer (pH 4.3) and isopropanol precipitation, tRNA was subjected to deacylation with 0.1 M Tris-HCl (pH 9.0) at 37 °C for 45 min. The pH was further decreased by the addition of 3 M NaOAc (pH 4.5) to its final concentration of 0.3 M. After isopropanol precipitation, uncharged tRNA was dissolved in nuclease-free water and dialyzed twice against 1000 volumes of ultrapure water.

SUPPLEMENTARY FIGURES

Figure S1. RP-HPLC data for BotA2 and BotCA purification

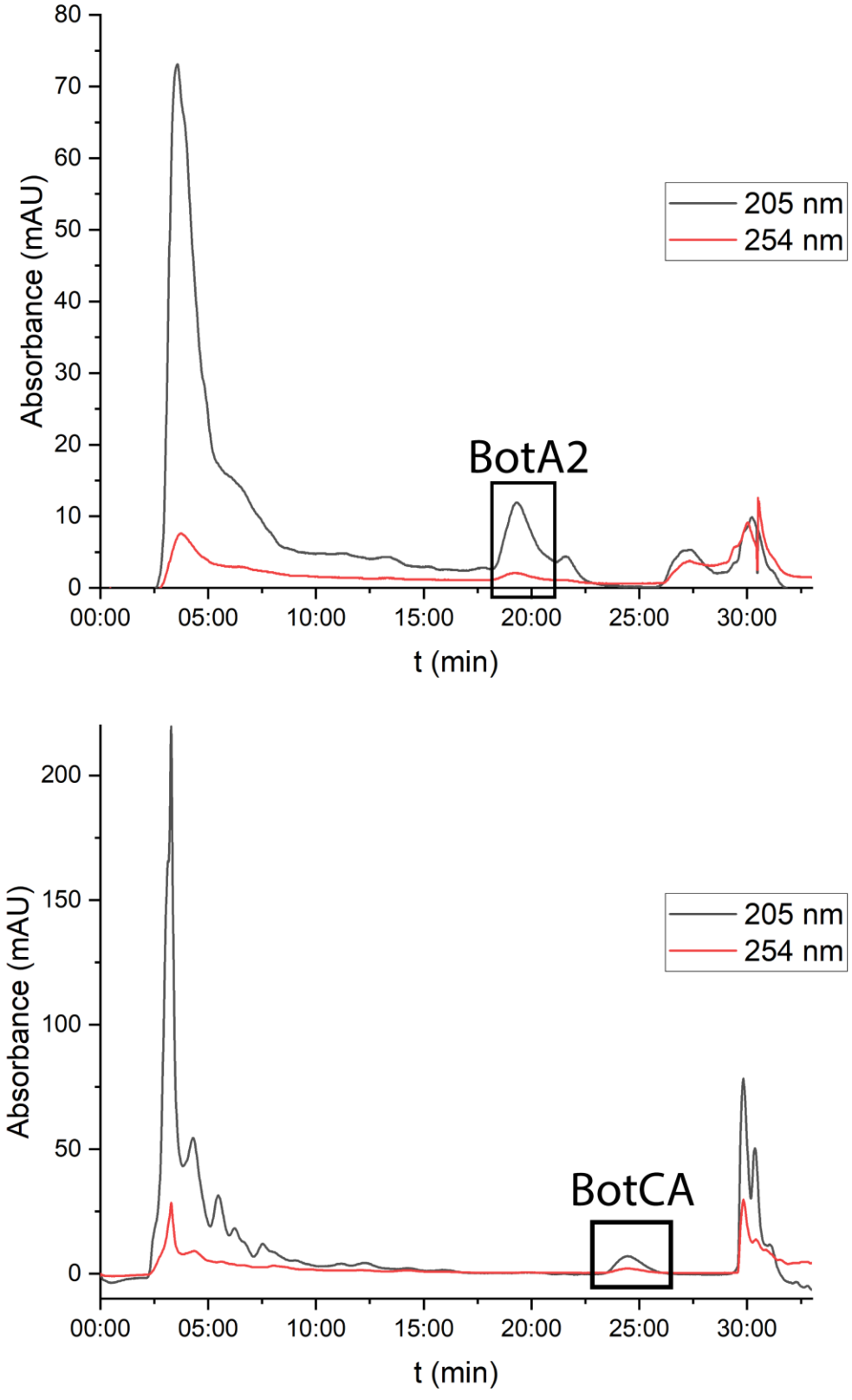

Figure S2. HRMS/MS fragmentation for BotA2 and BotCA

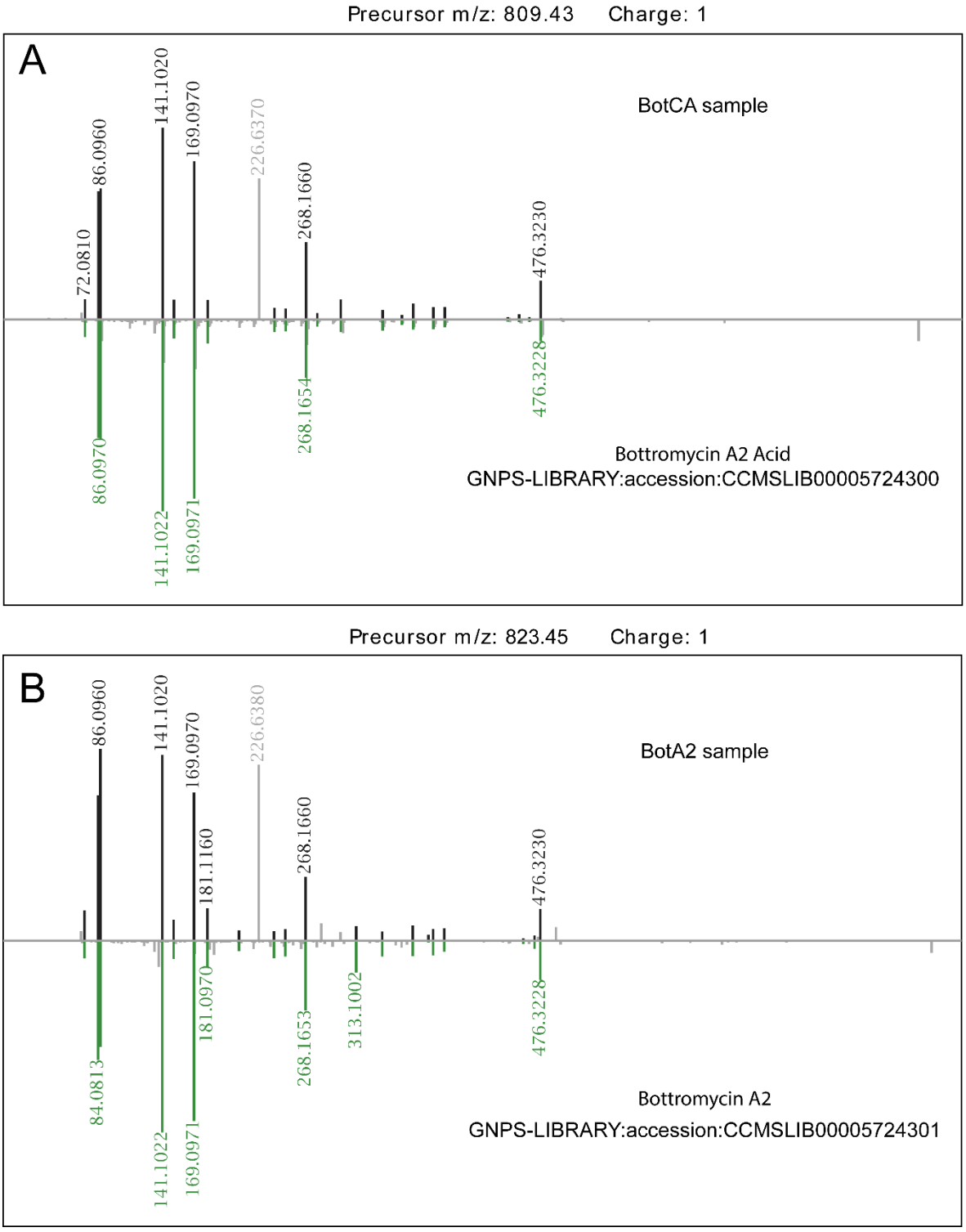

Comparison of the MS/MS fragmentation spectra of BotCA (A) and BotA2 (B), illustrated using the GNPS molecular networking platform [15]. The analysis was carried out for the $[M+H]^+$ adducts, with precursor masses indicated in the figure. The experimental fragmentation patterns were mirrored against reference spectra from the GNPS library: bottromycin A_2 acid (accession CCMSLIB00005724300) and bottromycin A_2 (accession CCMSLIB00005724301).

Figure S3. Inhibition of protein synthesis *in vitro* by BotA2 in a bacterial cell-free system

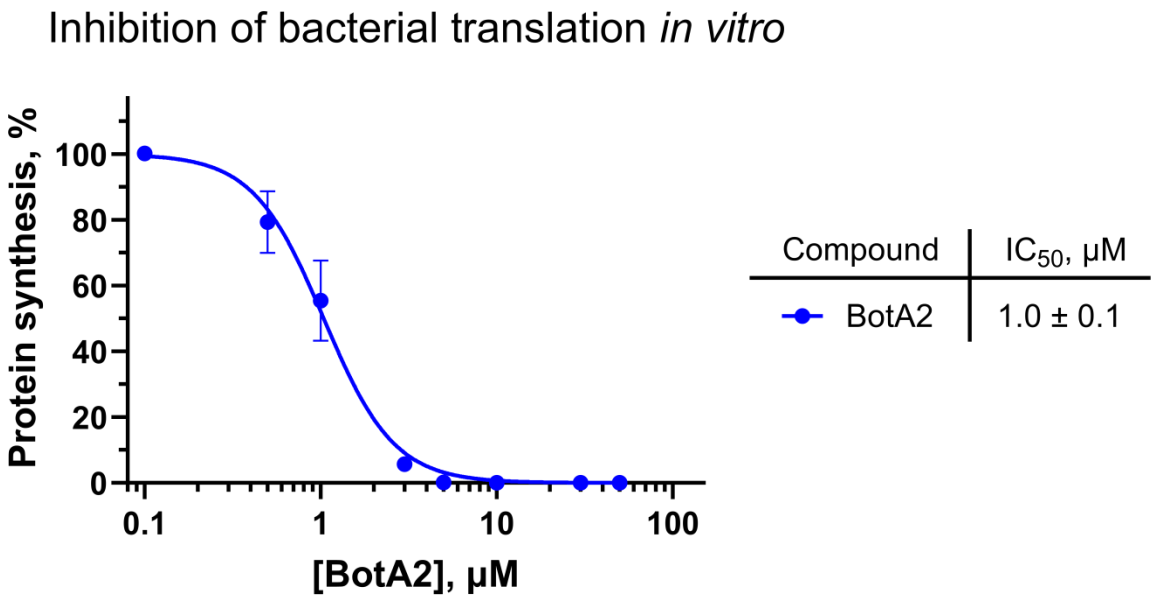

Inhibition of protein synthesis by increasing concentrations of bottromycin A_2 (BotA2) was asessed *in vitro* in a cell-free bacterial translation system using the commercially available *E. coli* S30 extract. The relative maximum Fluc accumulation rates are plotted *vs.* BotA2 concentration. Error bars represent standard deviation. All reactions were repeated at least two times. The calculated IC_{50} values and 95% confidence intervals are shown in the table.

Figure S4. Inhibition of protein synthesis *in vitro* by BotA2 and BotCA in HEK293T whole cell lysate system

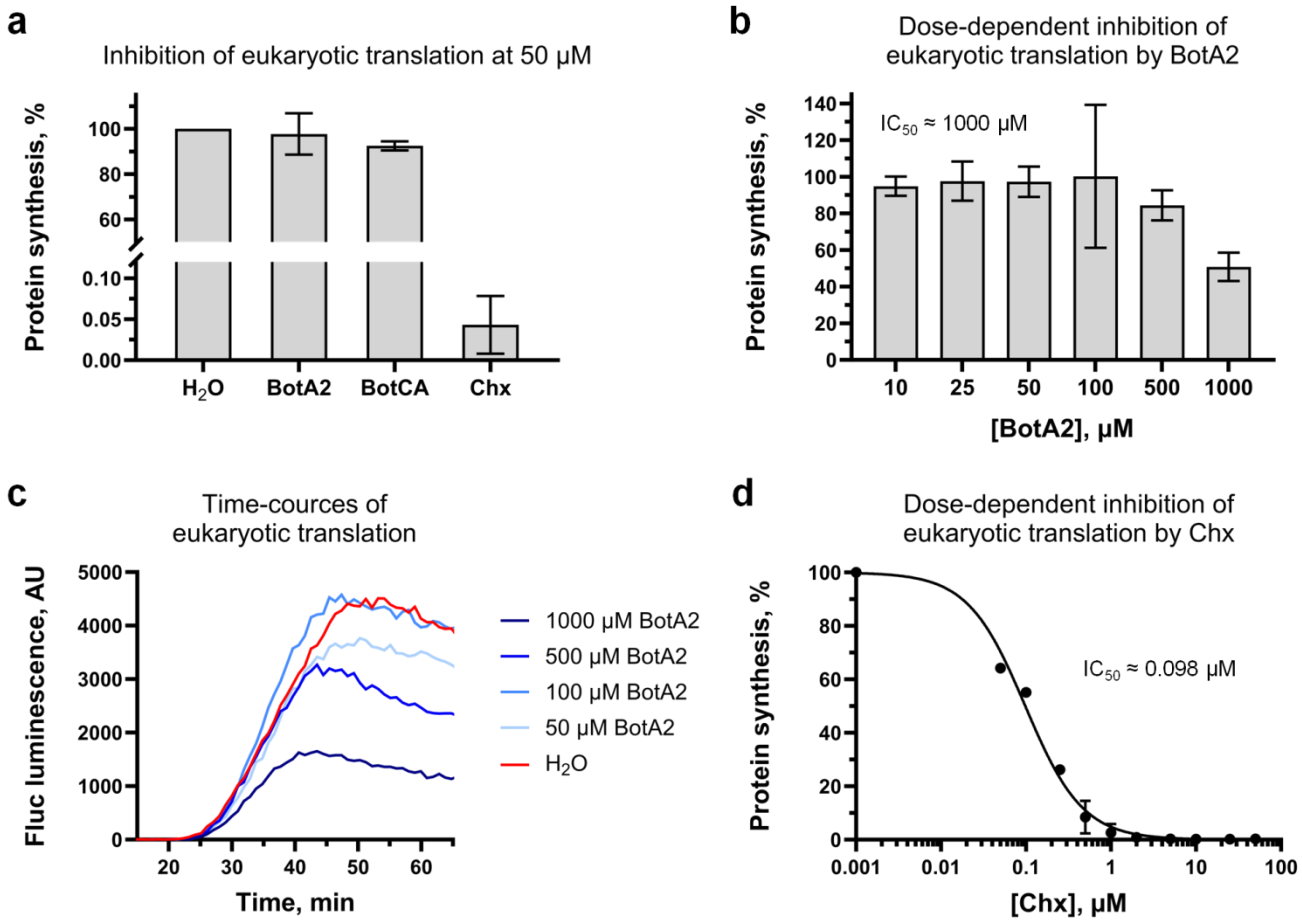

Inhibition of protein synthesis was assessed *in vitro* in a mammalian cell-free translation system based on HEK293T whole cell extracts. a) Inhibition of eukaryotic translation by BotA2 and BotCA, measured at 50 μM concentration. BotA2, bottromycin A_2. BotCA, bottromycin A_2 carboxylic acid. Chx, cycloheximide, was used as a reference agent. b) Dose-dependent inhibition of eukaryotic translation by BotA2. a,b) Relative maximum Fluc accumulation rates are shown. All reactions were repeated at least two times. c) Time-courses of Fluc activity accumulation in eukaryotic translation system upon treatment with different concentrations of BotA2. AU, arbitrary units. Please, note that luminescence values (AUs) are in the optimal detection range and do not approach the upper detection limit of the device (10,000,000 AU). d) Dose-dependent inhibition of eukaryotic translation by Chx. a,b,d) Error bars represent standard deviation.

Figure S5. Antibacterial activity of BotA2 against *Escherichia coli* cells carrying mutations in the 23S rRNA gene.

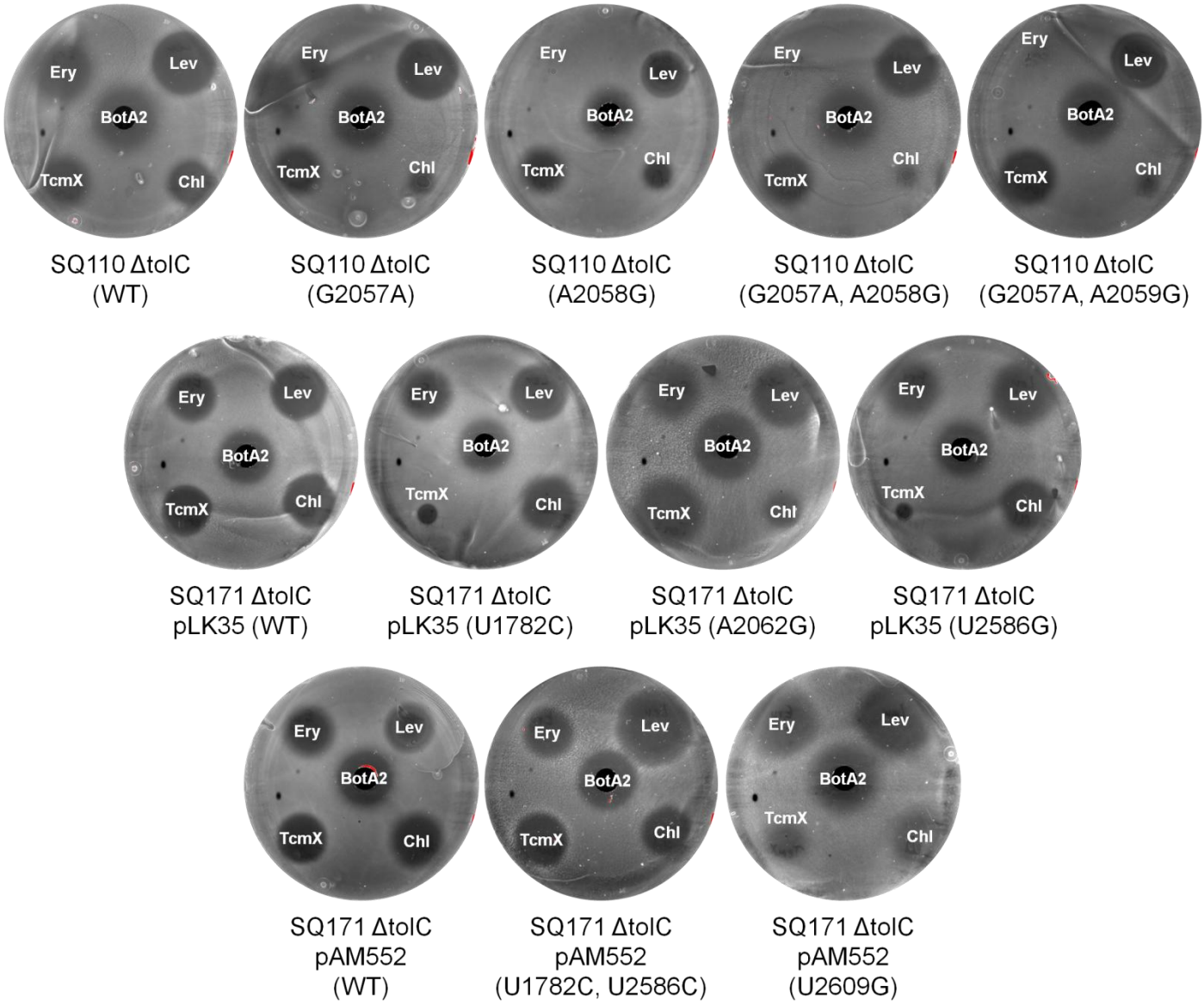

Agar diffusion assay reveals the activity of bottromycin A_2 (BotA2) against a panel of *E. coli* strains resistant to typical 50S-targeting antibiotics, such as erythromycin, tetracenomycin X, and chloramphenicol. Resistance is defined by point mutations in the 23S rRNA gene. The corresponding nucleotide substitutions are indicated in brackets. WT, wild-type 23S rRNA gene. The following antibiotics were applied on the surface of an agar plate coated with SQ110 ΔtolC or SQ171 ΔtolC cells: erythromycin (Ery, 5 µg), levofloxacin (Lev, 25 ng), tetracenomycin X (TcmX, 5 µg), chloramphenicol (Chl, 2 µg). In the center of each agar plate, a well was made and filled with 50 µL of 1 mM BotA2 dissolved in 30% acetonitrile aqueous.

Figure S6. Correlation analysis of *MaxStallProbability* scores between two independent Toe-seq experiments.

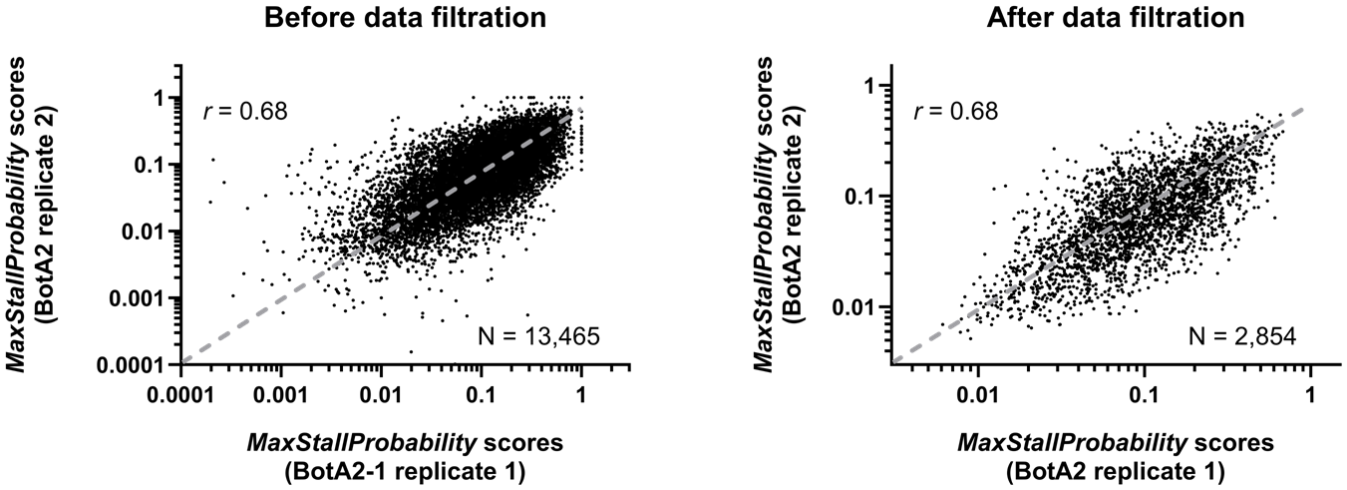

Toe-seq analysis of BotA2 was performed in two biological replicates. *MaxStallProbability* scores have been calculated to reveal antibiotic-specific ribosome stalling sites. A subset of mRNAs associated with coincident stalling sites (*StallPosition*) in two replicates was selected for correlation analysis. Only mRNAs with *MaxStallProbability* scores greater than 0 were considered. The number of such mRNAs (N) is presented on each plot. Spearman correlation coefficient (*r*) of the corresponding *MaxStallProbability* scores is presented on each plot, p-value < 0.0001 (two-tailed). The trend line is shown as a gray dashed line.

Figure S7. pLogo analysis of ribosome stalling sites with alanine fixed as the incoming A-site amino acid.

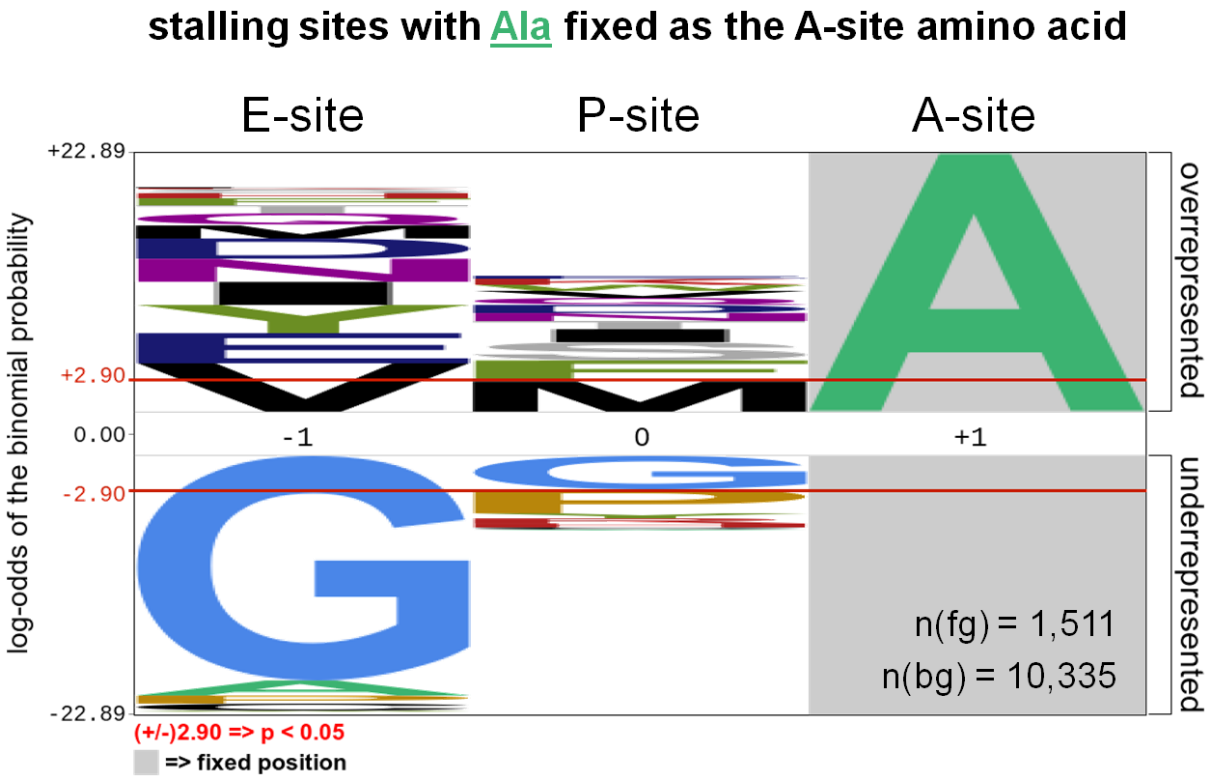

pLogo analysis of a subset of BotA2-induced ribosome stalling sites, in which alanine (Ala, A) is fixed as the incoming A-site amino acid (position +1). Amino acids corresponding to codons occupying the E- and P-sites of arrested ribosomes are indicated. The n(fg) and n(bg) values represent the number of foreground and background sequences used to generate the image, respectively. Red horizontal lines on the pLogo correspond to p-value = 0.05.

Figure S8. *MaxStallProbability* scores of AUG-XXX-GGC ribosome stalling sites, depending on the identity of the XXX codon.

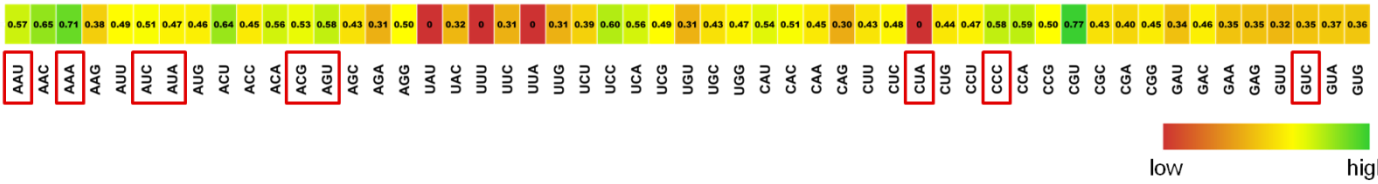

MaxStallProbability scores corresponding to different AUG-XXX-GGC ribosome stalling sites, where XXX is the second codon of the open reading frame (ORF) and does not encode Gly or Ala, are indicated within the cells of the heatmap. The values were calculated as the maximum among both Toe-seq datasets derived from BotA2-treated samples. A *MaxStallProbability* score of 0 means that the respective site was not found in both datasets. Red frames mark the codons selected for toe-printing analysis.

Figure S9. Toe-printing analysis of BotA2 on mRNAs encoding fMet-Gly-Phe peptide.

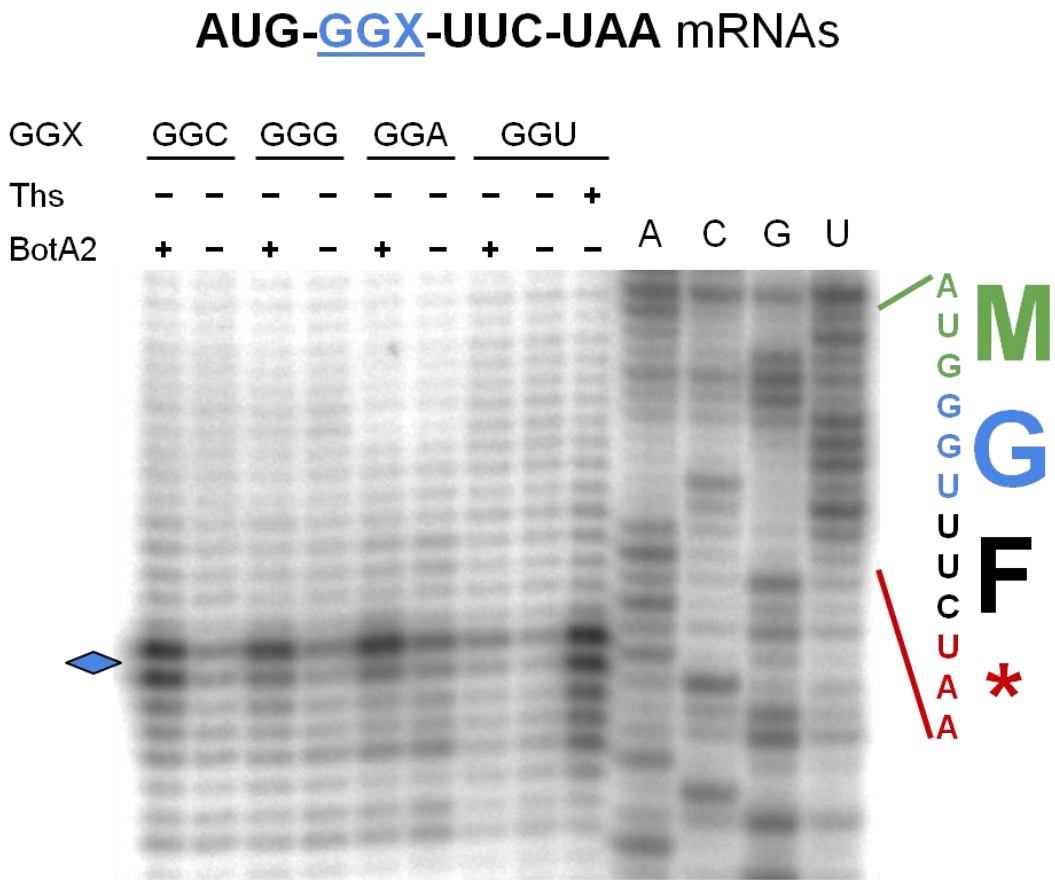

Toe-printing analysis of bottromycin A_2 (BotA2) on a set of short mRNA templates encoding fMet-Gly-Phe peptide. All four 3-nt Gly codons were tested to assess the efficiency of BotA2-induced ribosome stalling. Sequences of the corresponding ORF and the encoded amino acids are shown on the right. Asterisk (*) in the translated sequence denotes a stop codon. Blue diamond marks the toe-printing bands corresponding to BotA2-induced ribosome stalling. Thiostrepton (Ths) was included to map the translation start site. Antibiotics were added to the final concentration of 50 μM.

Figure S10. Accumulation of ppGpp in *E. coli* cells upon treatment with BotA2.

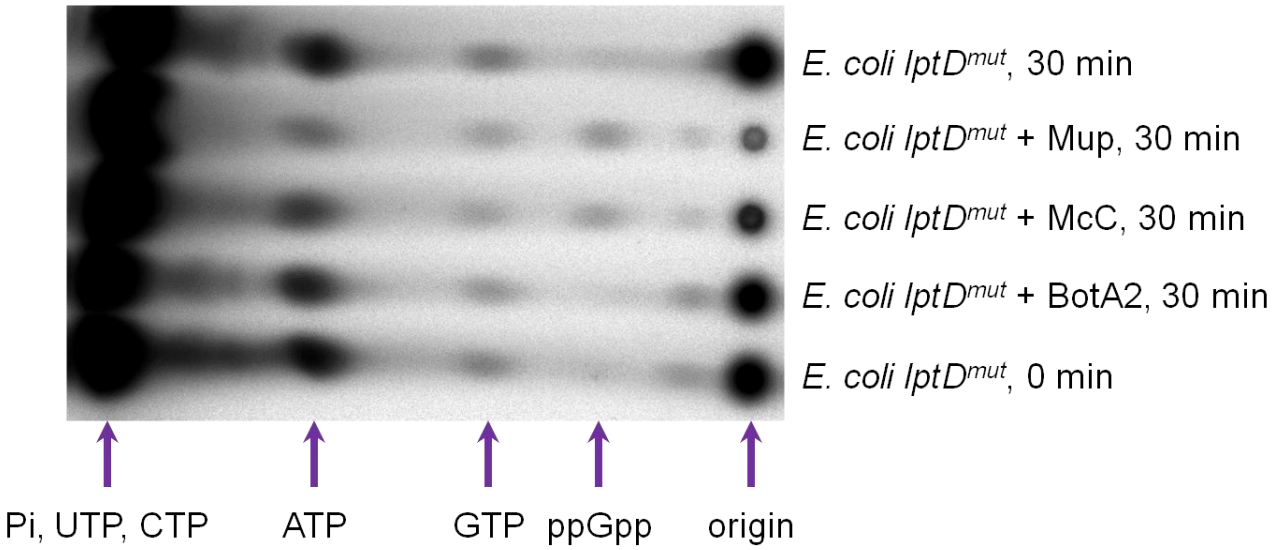

Thin-layer chromatography of [^{32}P]-labeled nucleotides isolated from *E. coli lptD*^{mut} after 30 min incubation with bottromycin A_2 (BotA2), microcin C (McC), or mupirocin (Mup). BotA2 and McC were added to the final concentration of 20 μM, while Mup was added to the final concentration of 60 μM.

Figure S11. Reporter assay for codon misreading by $tRNA^{Glu}$.

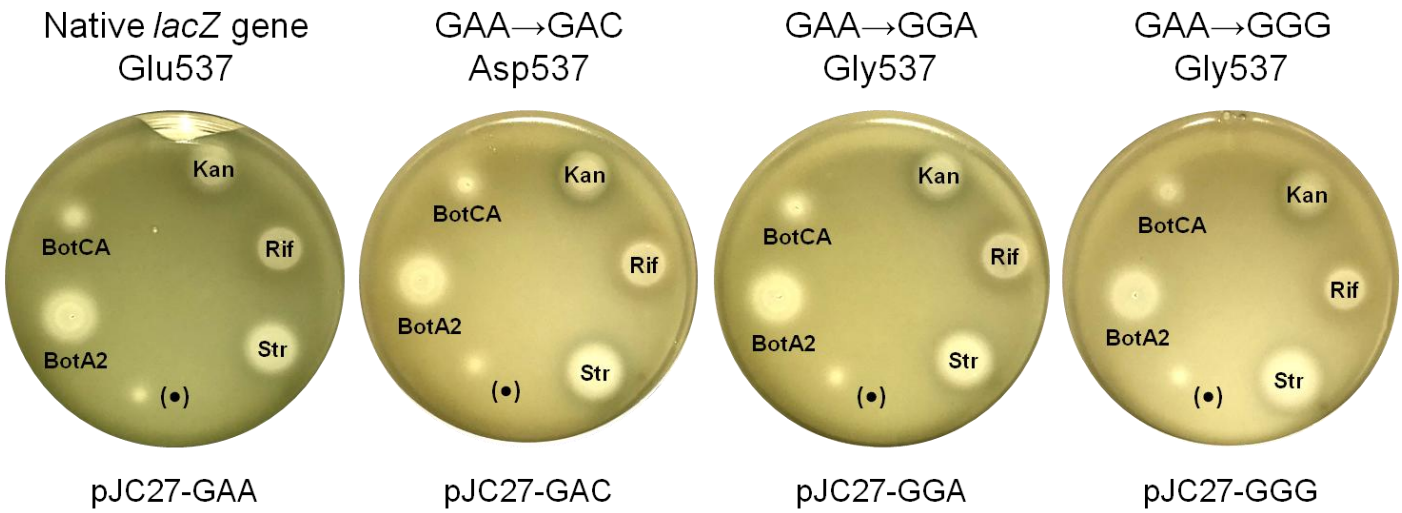

Bottromycin A_2 (BotA2) does not cause misreading of the 537th Gly codon of the mutated β-galactosidase gene by Glu-$tRNA^{Glu}$ in *E. coli ΔtolC* cells transformed with reporter systems. The pJC27-GAA construct harbors the native β-galactosidase gene (*lacZ*), in which Glu537 is a catalytic residue essential for the enzymatic degradation of the X-Gal substrate. Constructs pJC27-GAC, pJC27-GGA, and pJC27-GGG harbor mutant variants of the *lacZ* with the 537th GAA codon replaced by GAC, GGA, or GGG, respectively. Miscoding agents, such as kanamycin and streptomycin, reduce the fidelity of translation allowing Glu to be incorporated into the polypeptide sequence at the 537th position of mutated *lacZ* variants. The appearance of blue coloration along the edge of the growth inhibition zone indicates that the antibiotic causes translation errors (mistranslation). The following antibiotics were applied on the surface of agar plates coated with *E. coli ΔtolC* cells transformed with the indicated pJC27 plasmids: kanamycin (Kan, 5 μg), rifampicin (Rif, 10 μg), streptomycin (Str, 5 μg), bottromycin A_2 carboxylic acid (BotCA, 16.2 μg), bottromycin A_2 (BotA2, 16.5 μg), and bottromycin A_2 (indicated as (●), 0.4 μg). Note that BotCA exhibits smaller growth inhibition zones compared to BotA2, probably due to its impaired penetration into bacterial cells.

Figure S12. Comparison of size exclusion chromatography profiles of BotA2-treated and untreated ribosomal complexes.

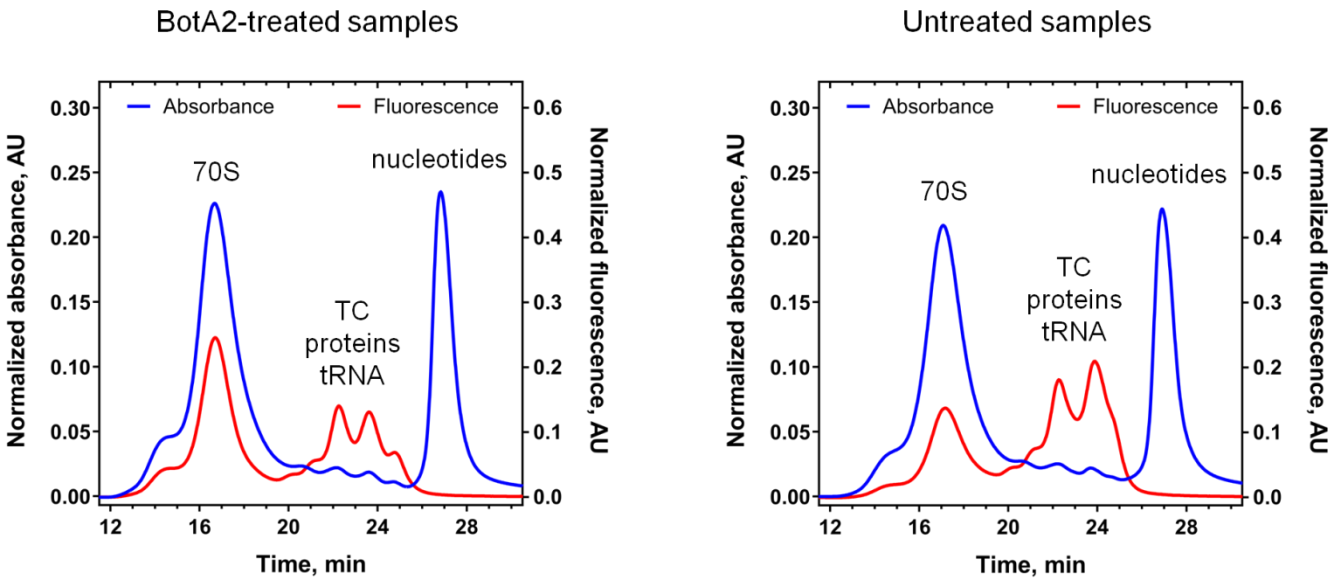

Profiles of size exclusion chromatography of the 70S initiation complex after incubation with the ternary complex Gly-tRNA^{Gly}(Prf16/17/20)·EF-Tu·GTP in the presence or absence of 100 μM BotA2. Absorbance values were measured at 260 nm (blue). Fluorescence was measured using excitation at 460 nm and detection at 510 nm (red). TC, ternary complexes.

Figure S13. Codon-anticodon base-pairing involved in the recognition of Gly codons.

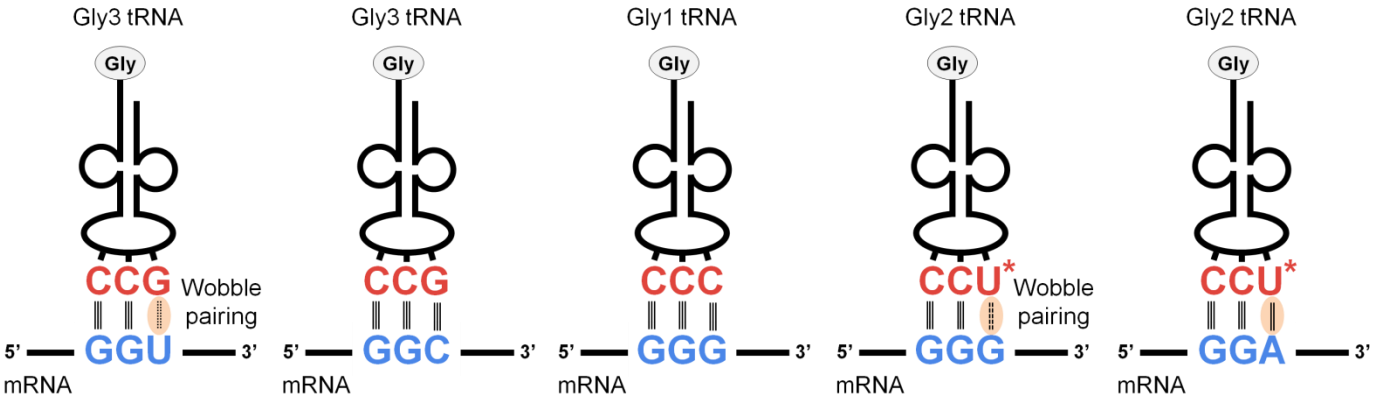

Schematic representation showing the formation of codon-anticodon complexes between Gly codons and cognate Gly-tRNA^{Gly}. The canonical Watson–Crick base pairing is shown by vertical lines. Dotted lines represent a wobble base pairing. Dashed lines indicate a wobble base pairing additionally stabilized with a modified uracil (U*). The number of lines reflects the number of hydrogen bonds. Asterisk in the anticodon triplet (U*) indicates a 5-methylaminomethyl modification of the wobble uridine (mnm^{5}U). Pale orange area highlights weak base pairs at the 3rd poition.

.

SUPPLEMENTARY TABLES

Table S1. Primers used for the synthesis of DNA templates.

Primer name	Nucleotide sequence (5' to 3')
RST1-fwd	AC**TAATACGACTCACTATAGGG**CTTAAGTATAAGGAGGAAAACATA TGTATTGGGTAACCTCACGTCAGCCGAATATGCTGAAAATCCATGG CT
RST1-rev	GGTTATAATGAATTTTGCTTATTAACGATAGAATTCTATCACTTTTTT TATTATTATTAGGCGCAGTCTTCGAAGCCATGGATTTTCAGC
RST3-fwd	AC**TAATACGACTCACTATAGGG**CTTAAGTATAAGGAGGAAAACATA TGCATTCTAAATATATATGGGTACTGCGTCAGCCGAATATGAAAGG CTTCG
RST3-rev	GGTTATAATGAATTTTGCTTATTAACGATAGAATTCTATCACATTCTT GATTCTTATTAGGCGGTGCAGTCTTCGAAGCCTTTCATATTCG
NV1	GGTTATAATGAATTTTGCTTATTAAC
M-AGT-GGC	ATGCA**TAATACGACTCACTATAGGG**CTTAAGTATAAGGAGGAAAAC ATATGAGTGGCTAAGAGACGGACGAGAGCGGC
M-GTC-GGC	ATGCA**TAATACGACTCACTATAGGG**CTTAAGTATAAGGAGGAAAAC ATATGGTCGGCTAAGAGACGGACGAGAGCGGC
M-ATC-GGC	ATGCA**TAATACGACTCACTATAGGG**CTTAAGTATAAGGAGGAAAAC ATATGATCGGCTAAGAGACGGACGAGAGCGGC
M-AAT-GGC	ATGCA**TAATACGACTCACTATAGGG**CTTAAGTATAAGGAGGAAAAC ATATGAATGGCTAAGAGACGGACGAGAGCGGC
M-ACG-GGC	ATGCA**TAATACGACTCACTATAGGG**CTTAAGTATAAGGAGGAAAAC ATATGACGGGCTAAGAGACGGACGAGAGCGGC
M-ATA-GGC	ATGCA**TAATACGACTCACTATAGGG**CTTAAGTATAAGGAGGAAAAC ATATGATAGGCTAAGAGACGGACGAGAGCGGC
M-CTA-GGC	ATGCA**TAATACGACTCACTATAGGG**CTTAAGTATAAGGAGGAAAAC ATATGCTAGGCTAAGAGACGGACGAGAGCGGC
M-CCC-GGC	ATGCA**TAATACGACTCACTATAGGG**CTTAAGTATAAGGAGGAAAAC ATATGCCCGGCTAAGAGACGGACGAGAGCGGC
M-AAA-GGC	ATGCA**TAATACGACTCACTATAGGG**CTTAAGTATAAGGAGGAAAAC ATATGAAAGGCTAAGAGACGGACGAGAGCGGC
M-AGT-GGC-F	ATGCA**TAATACGACTCACTATAGGG**CTTAAGTATAAGGAGGAAAAC ATATGAGTGGCTTCTAAGAGACGGACGAGAGCGGC

M-AGT-GGG-F	ATGCA**TAATACGACTCACTATAGGG**CTTAAGTATAAGGAGGAAAAC ATATGAGTGGGTTCTAAGAGACGGACGAGAGCGGC
M-AGT-GGA-F	ATGCA**TAATACGACTCACTATAGGG**CTTAAGTATAAGGAGGAAAAC ATATGAGTGGATTCTAAGAGACGGACGAGAGCGGC
M-AGT-GGT-F	ATGCA**TAATACGACTCACTATAGGG**CTTAAGTATAAGGAGGAAAAC ATATGAGTGGTTTCTAAGAGACGGACGAGAGCGGC
M-GGC-F	ATGCA**TAATACGACTCACTATAGGG**CTTAAGTATAAGGAGGAAAAC ATATGGGCTTCTAAGAGACGGACGAGAGCGGC
M-GGG-F	ATGCA**TAATACGACTCACTATAGGG**CTTAAGTATAAGGAGGAAAAC ATATGGGGTTCTAAGAGACGGACGAGAGCGGC
M-GGA-F	ATGCA**TAATACGACTCACTATAGGG**CTTAAGTATAAGGAGGAAAAC ATATGGGATTCTAAGAGACGGACGAGAGCGGC
M-GGT-F	ATGCA**TAATACGACTCACTATAGGG**CTTAAGTATAAGGAGGAAAAC ATATGGGTTTCTAAGAGACGGACGAGAGCGGC
M-AGT	ATGCA**TAATACGACTCACTATAGGG**CTTAAGTATAAGGAGGAAAAC ATATGAGTTAAGAGACGGACGAGAGCGGC
M-GGC	ATGCA**TAATACGACTCACTATAGGG**CTTAAGTATAAGGAGGAAAAC ATATGGGCTAAGAGACGGACGAGAGCGGC
CER-R	GCGTTAAGGCTATGTACGGAACAGCTCCTCGCCCTTG
NEW-CER-R	GCGTTAAGGCTATGTACGCGCCGTCCAGCTCGACCAGG
NV2	GCGTTAAGGCTATGTAC
T7-fwd-1	ATGCA**TAATACGACTCACTATAGGG**
T7-fwd-2	CGAATT**TAATACGACTCACTATAGG**
LP-rev	GCTTGCATGCCTGCAGACGCA

The sequence of the T7 promoter is marked in bold; the sequence of the NV1 primer used for reverse transcription is underlined; the sequence of the NV2 primer used for reverse transcription is underlined twice.

Table S2. Sequences of DNA templates used in this work

DNA template	Nucleotide sequence (5’ to 3’)
RST1	AC**TAATACGACTCACTATAGGG**CTTAAGTATAAGGAGGAAAACA TATGTATTGGGTAACCTCACGTCAGCCGAATATGCTGAAAATCCA TGGCTTCGAAGACTGCGCCTAATAATAATAAAAAAAGTGATAGAA TTCTATC**GTTAATAAGCAAAATTCATTATAACC**
RST3	AC**TAATACGACTCACTATAGGG**CTTAAGTATAAGGAGGAAAACA TATGCATTCTAAATATATATGGGTACTGCGTCAGCCGAATATGAA AGGCTTCGAAGACTGCACCGCCTAATAAGAATCAAGAATGTGAT AGAATTCTATC**GTTAATAAGCAAAATTCATTATAACC**
M-AGT-GGC (fMet-Ser-Gly)	ATGCA**TAATACGACTCACTATAGGG**CTTAAGTATAAGGAGGAAA ACATATGAGTGGCTAAGAGACGGACGAGAGCGGCCTGGTGAGC AAGGGCGAGGAGCTGTTCC**GTACATAGCCTTAACGC**
M-GTC-GGC (fMet-Val-Gly)	ATGCA**TAATACGACTCACTATAGGG**CTTAAGTATAAGGAGGAAA ACATATGGTCGGCTAAGAGACGGACGAGAGCGGCCTGGTGAGC AAGGGCGAGGAGCTGTTCC**GTACATAGCCTTAACGC**
M-ATC-GGC (fMet-Ile-Gly)	ATGCA**TAATACGACTCACTATAGGG**CTTAAGTATAAGGAGGAAA ACATATGATCGGCTAAGAGACGGACGAGAGCGGCCTGGTGAGC AAGGGCGAGGAGCTGTTCC**GTACATAGCCTTAACGC**
M-AAT-GGC (fMet-Asn-Gly)	ATGCA**TAATACGACTCACTATAGGG**CTTAAGTATAAGGAGGAAA ACATATGAATGGCTAAGAGACGGACGAGAGCGGCCTGGTGAGC AAGGGCGAGGAGCTGTTCC**GTACATAGCCTTAACGC**
M-ACG-GGC (fMet-Thr-Gly)	ATGCA**TAATACGACTCACTATAGGG**CTTAAGTATAAGGAGGAAA ACATATGACGGGCTAAGAGACGGACGAGAGCGGCCTGGTGAGC AAGGGCGAGGAGCTGTTCC**GTACATAGCCTTAACGC**
M-ATA-GGC (fMet-Ile-Gly)	ATGCA**TAATACGACTCACTATAGGG**CTTAAGTATAAGGAGGAAA ACATATGATAGGCTAAGAGACGGACGAGAGCGGCCTGGTGAGC AAGGGCGAGGAGCTGTTCC**GTACATAGCCTTAACGC**

M-CTA-GGC (fMet-Leu-Gly)	ATGCA**TAATACGACTCACTATAGGG**CTTAAGTATAAGGAGGAAA ACATATGCTAGGCTAAGAGACGGACGAGAGCGGCCTGGTGAGC AAGGGCGAGGAGCTGTTCC**GTACATAGCCTTAACGC**
M-CCC-GGC (fMet-Pro-Gly)	ATGCA**TAATACGACTCACTATAGGG**CTTAAGTATAAGGAGGAAA ACATATGCCCGGCTAAGAGACGGACGAGAGCGGCCTGGTGAGC AAGGGCGAGGAGCTGTTCC**GTACATAGCCTTAACGC**
M-AAA-GGC (fMet-Lys-Gly)	ATGCA**TAATACGACTCACTATAGGG**CTTAAGTATAAGGAGGAAA ACATATGAAAGGCTAAGAGACGGACGAGAGCGGCCTGGTGAGC AAGGGCGAGGAGCTGTTCC**GTACATAGCCTTAACGC**
M-AGT-GGC-F (fMet-Ser-Gly-Phe)	ATGCA**TAATACGACTCACTATAGGG**CTTAAGTATAAGGAGGAAA ACATATGAGTGGCTTCTAAGAGACGGACGAGAGCGGCCTGGTG AGCAAGGGCGAGGAGCTGTTCC**GTACATAGCCTTAACGC**
M-AGT-GGG-F (fMet-Ser-Gly-Phe)	ATGCA**TAATACGACTCACTATAGGG**CTTAAGTATAAGGAGGAAA ACATATGAGTGGGTTCTAAGAGACGGACGAGAGCGGCCTGGTG AGCAAGGGCGAGGAGCTGTTCC**GTACATAGCCTTAACGC**
M-AGT-GGA-F (fMet-Ser-Gly-Phe)	ATGCA**TAATACGACTCACTATAGGG**CTTAAGTATAAGGAGGAAA ACATATGAGTGGATTCTAAGAGACGGACGAGAGCGGCCTGGTGA GCAAGGGCGAGGAGCTGTTCC**GTACATAGCCTTAACGC**
M-AGT-GGT-F (fMet-Ser-Gly-Phe)	ATGCA**TAATACGACTCACTATAGGG**CTTAAGTATAAGGAGGAAA ACATATGAGTGGTTTCTAAGAGACGGACGAGAGCGGCCTGGTGA GCAAGGGCGAGGAGCTGTTCC**GTACATAGCCTTAACGC**
M-GGC-F (fMet-Gly-Phe)	ATGCA**TAATACGACTCACTATAGGG**CTTAAGTATAAGGAGGAAA ACATATGGGCTTCTAAGAGACGGACGAGAGCGGCCTGGTGAGC AAGGGCGAGGAGCTGTTCC**GTACATAGCCTTAACGC**
M-GGG-F (fMet-Gly-Phe)	ATGCA**TAATACGACTCACTATAGGG**CTTAAGTATAAGGAGGAAA ACATATGGGGTTCTAAGAGACGGACGAGAGCGGCCTGGTGAGC AAGGGCGAGGAGCTGTTCC**GTACATAGCCTTAACGC**
M-GGA-F	ATGCA**TAATACGACTCACTATAGGG**CTTAAGTATAAGGAGGAAA

(fMet-Gly-Phe)	ACATATGGGATTCTAAGAGACGGACGAGAGCGGCCTGGTGAGC AAGGGCGAGGAGCTGTTCC**GTACATAGCCTTAACGC**
M-GGT-F (fMet-Gly-Phe)	ATGCA**TAATACGACTCACTATAGGG**CTTAAGTATAAGGAGGAAA ACATATGGGTTTCTAAGAGACGGACGAGAGCGGCCTGGTGAGC AAGGGCGAGGAGCTGTTCC**GTACATAGCCTTAACGC**
M-AGT (fMet-Ser)	ATGCA**TAATACGACTCACTATAGGG**CTTAAGTATAAGGAGGAAA ACATATGAGTTAAGAGACGGACGAGAGCGGCCTGGTGAGCAAG GGCGAGGAGCTGTTCC**GTACATAGCCTTAACGC**
MG (fMet-Gly)	ATGCA**TAATACGACTCACTATAGGG**CTTAAGTATAAGGAGGAAA ACATATGGGCTAAGAGACGGACGAGAGCGGCCTGGTGAGCAAG GGCGAGGAGCTGTTCACCGGGGTGGTGCCCATCCTGGTCGAGC TGGACGGCGC**GTACATAGCCTTAACGC**
MF (fMet-Phe-…)	CGAATT**TAATACGACTCACTATAGGG**AATTCAAAAATTTAAAAGT TAACAGGTATACATACTATGTTTACGATTACTACGATCTTCTTCAC TTAATGCGTCTGCAGGCATGCAAGC
MV (fMet-Val-…)	CGAATT**TAATACGACTCACTATAGGG**AATTCAAAAATTTAAAAGT TAACAGGTATACATACTATGGTTTTTATTACTACGATCTTCTTCAC TTAATGCGTCTGCAGGCATGCAAGC

The sequence of the T7 promoter and sequences complementary to either the NV1 or the NV2 primers are marked in bold. Coding sequences are underlined.

Table S3. Parameters of Toe-seq datasets

Raw datasets, **before** normalization to controls	
Total number of unique mRNAs in all 4 datasets	57,972
Total number of mRNAs in the BotA2-1 dataset (BotA2 replicate 1)	56,687
Total number of mRNAs in the BotA2-2 dataset (BotA2 replicate 2)	56,431
Total number of mRNAs in the Control-1 dataset (Control replicate 1)	55,835
Total number of mRNAs in the Control-2 dataset (Control replicate 2)	56,089
Total number of mapped reads in the BotA2-1 dataset (BotA2 replicate 1)	9,903,509
Total number of mapped reads in the BotA2-2 dataset (BotA2 replicate 2)	9,360,524
Total number of mapped reads in the Control-1 dataset (Control replicate 1)	6,148,055
Total number of mapped reads in the Control-2 dataset (Control replicate 2)	5,923,640
Datasets **after** normalization to controls, **before** filtering the data	
Total number of unique mRNAs in 2 datasets (BotA2 replicates 1 and 2)	56,243
Total number of mRNAs in the BotA2-1 dataset (BotA2 replicate 1)	55,292
Total number of mRNAs in the BotA2-2 dataset (BotA2 replicate 2)	55,387
Number of shared mRNAs between two datasets (BotA2 replicates 1 and 2)	54,436
Number of mRNAs with coincident stalling sites in two datasets (BotA2 replicates 1 and 2)	13,290
Datasets **after** normalization to controls and **after** filtering the data	
Total number of unique mRNAs in 2 datasets (BotA2 replicates 1 and 2)	24,156

Total number of mRNAs in the BotA2-1 dataset (BotA2 replicate 1)	15,995
Total number of mRNAs in the BotA2-2 dataset (BotA2 replicate 2)	15,694
Number of shared mRNAs between two datasets (BotA2 replicates 1 and 2)	7,533
Number of mRNAs with coincident stalling sites between two datasets (BotA2 replicates 1 and 2)	2,854

Table S4. Antibacterial activity of BotA2 against chloramphenicol-resistant bacterial strains

	Compound, minimum inhibitory concentration (MIC), μM		
Strain	BotA2	BotCA	Chl
E. coli lptD^{mut} [a]	6.25	25	200
B. subtilis 168 [b]	0.78-1.56	nt	12.5
B. subtilis 168 pHT01-cat [c]	0.78-1.56	nt	200
B. subtilis 168 pHT01-cfr [d]	1.56-3.13	nt	100

[a] *E. coli lptD*^{mut}: chloramphenicol-resistant strain due to the constitutive expression of the *cat* gene, which encodes a chloramphenicol acetyltransferase, CAT.

[b] *B. subtilis* 168: chloramphenicol-susceptible strain.

[c] *B. subtilis* 168 pHT01-cat: chloramphenicol-resistant strain due to the constitutive expression of the *cat* gene, which encodes a chloramphenicol acetyltransferase, CAT.

[d] *B. subtilis* 168 pHT01-cfr: chloramphenicol-resistant strain due to the constitutive expression of the *cfr* gene, which encodes a methyltransferase that modifies A2503 residue of the 23S rRNA.

At least two replicates of MIC measurements were performed.

nt, not tested.

Table S5. Characteristics of Gly codons and tRNAs^{Gly} in *Escherichia coli* cells.

Characteristics of Gly codons in *E. coli* cells						
Codon	tRNA^{Gly}	Codon usage in genome, % [16]	Codon usage in transcriptome, % [17]	RSCU, [18]	CEI, [19]	CP, [19]
GGU	Gly3	2.37	3.62	2.28	14.96	698 ± 65
GGC	Gly3	2.06	2.97	1.65	4.35	514 ± 50
GGG	Gly1 Gly2	1.23	0.92	0.04	-13.39	226 ± 19
GGA	Gly2	1.36	0.63	0.02	-15.15	229 ± 19

Characteristics of tRNA^{Gly} in *E. coli* cells					
tRNA^{Gly}	Anticodon	Anticodon modifications [20]	Number of tRNA genes [21]	Intracellular concentration of tRNA, μM [17]	Intracellular concentration of free ternary complexes, μM [17]
Gly1	CCC	–	1	4.43	3.44-3.51
Gly2	UCC	mnm^{5}U	1	6.65	4.51-4.70
Gly3	GCC	–	4	24.96	14.33-15.38

RSCU, relative synonymous codon usage. RSCU values were calculated for highly expressed genes to represent the codon frequency normalized to the expected frequency under the assumption of equal usage of the synonymous codons for Gly amino acid [18].

CEI, codon expression index. CEI shows the level of statistical significance of the correlation between the frequency of a certain codon occurrence in *E. coli* genes and the expression level of the corresponding protein [19]. In other words, CEI reflects if a certain codon has a tendency to be overrepresented in highly expressed genes.

CP, codon productivity [19]. CP shows the average amount of amino acids used by *E. coli* cells for protein production based on a certain codon. CP depends on a codon identity and corresponding tRNA frequencies.

mnm^5U, 5-methylaminomethyluridine.

SUPPLEMENTARY REFERENCES

1. Osterman, I. A., Wieland, M., Maviza, T. P., Lashkevich, K. A., Lukianov, D. A., Komarova, E. S., Zakalyukina, Y. V., Buschauer, R., Shiriaev, D. I., Leyn, S. A., Zlamal, J. E., Biryukov, M. V., Skvortsov, D. A., Tashlitsky, V. N., Polshakov, V. I., Cheng, J., Polikanov, Y. S., Bogdanov, A. A., Osterman, A. L., Dmitriev, S. E., et al. (2020) Tetracenomycin X inhibits translation by binding within the ribosomal exit tunnel, *Nature chemical biology*, **16**, 1071–1077, doi: https://doi.org/10.1038/s41589-020-0578-x.
2. Yagmurov, E., Tsibulskaya, D., Livenskyi, A., Serebryakova, M., Wolf, Y. I., Borukhov, S., Severinov, K., and Dubiley, S. (2020) Histidine-Triad Hydrolases Provide Resistance to Peptide-Nucleotide Antibiotics, *mBio*, **11**, e00497-00420, doi: https://doi.org/10.1128/mBio.00497-20.
3. Orelle, C., Carlson, S., Kaushal, B., Almutairi, M. M., Liu, H., Ochabowicz, A., Quan, S., Pham, V. C., Squires, C. L., Murphy, B. T., and Mankin, A. S. (2013) Tools for characterizing bacterial protein synthesis inhibitors, *Antimicrobial agents and chemotherapy*, **57**, 5994–6004, doi: https://doi.org/10.1128/AAC.01673-13.
4. Datsenko, K. A., and Wanner, B. L. (2000) One-step inactivation of chromosomal genes in *Escherichia coli* K-12 using PCR products, *Proceedings of the National Academy of Sciences of the United States of America*, **97**, 6640–6645, doi: https://doi.org/10.1073/pnas.120163297.
5. Baba, T., Ara, T., Hasegawa, M., Takai, Y., Okumura, Y., Baba, M., Datsenko, K. A., Tomita, M., Wanner, B. L., and Mori, H. (2006) Construction of *Escherichia coli* K-12 in-frame, single-gene knockout mutants: the Keio collection, *Molecular systems biology*, **2**, 2006.0008, doi: https://doi.org/10.1038/msb4100050.
6. Manickam, N., Joshi, K., Bhatt, M. J., and Farabaugh, P. J. (2016) Effects of tRNA modification on translational accuracy depend on intrinsic codon-anticodon strength, *Nucleic acids research*, **44**, 1871–1881, doi: https://doi.org/10.1093/nar/gkv1506.
7. Polikanov, Y. S., Szal, T., Jiang, F., Gupta, P., Matsuda, R., Shiozuka, M., Steitz, T. A., Vazquez-Laslop, N., and Mankin, A. S. (2014) Negamycin interferes with decoding and translocation by simultaneous interaction with rRNA and tRNA, *Molecular cell*, **56**, 541–550, doi: https://doi.org/10.1016/j.molcel.2014.09.021.
8. Orelle, C., Carlson, E. D., Szal, T., Florin, T., Jewett, M. C., and Mankin, A. S. (2015) Protein synthesis by ribosomes with tethered subunits, *Nature*, **524**, 119–124, doi: https://doi.org/10.1038/nature14862.
9. Pavlova, J. A., Khairullina, Z. Z., Tereshchenkov, A. G., Nazarov, P. A., Lukianov, D. A., Volynkina, I. A., Skvortsov, D. A., Makarov, G. I., Abad, E., Murayama, S. Y., Kajiwara, S., Paleskava, A., Konevega, A. L., Antonenko, Y. N., Lyakhovich, A., Osterman, I. A., Bogdanov, A. A., and Sumbatyan, N. V. (2021) Triphenilphosphonium Analogs of Chloramphenicol as Dual-Acting Antimicrobial and Antiproliferating Agents, *Antibiotics*, **10**, 489, doi: https://doi.org/10.3390/antibiotics10050489.

10. Wiegand, I., Hilpert, K., and Hancock, R. E. (2008) Agar and broth dilution methods to determine the minimal inhibitory concentration (MIC) of antimicrobial substances, *Nature protocols*, **3**, 163–175, doi: https://doi.org/10.1038/nprot.2007.521.
11. Terenin, I. M., Andreev, D. E., Dmitriev, S. E., and Shatsky, I. N. (2013) A novel mechanism of eukaryotic translation initiation that is neither m^7G-cap-, nor IRES-dependent, *Nucleic acids research*, **41**, 1807–1816, doi: https://doi.org/10.1093/nar/gks1282.
12. Kabilov, M. R., Komarova, E. S., Pichkur, E. B., Zotova, P. A., Kasatsky, P. S., Volynkina, I. A., Tupikin, A. E., Pavlova, J. A., Lukianov, D. A., Osterman, I. A., Pyshniy, D. V., Paleskava, A., Bogdanov, A. A., Dontsova, O. A., Konevega, A. L., and Sergiev, P. V. (2024) Context Specificity of Translation Inhibitors Revealed by Toe-seq, *Research Square*, doi: https://doi.org/10.21203/rs.3.rs-3832009/v1.
13. O'Shea, J. P., Chou, M. F., Quader, S. A., Ryan, J. K., Church, G. M., and Schwartz, D. (2013) pLogo: a probabilistic approach to visualizing sequence motifs, *Nature methods*, **10**, 1211–1212, doi: https://doi.org/10.1038/nmeth.2646.
14. Shapovalova, K. S., Zatonsky, G. V., Razumova, E. A., Ipatova, D. A., Lukianov, D. A., Sergiev, P. V., Grammatikova, N. E., Tikhomirov, A. S., and Shchekotikhin, A. E. (2024) Synthesis and Antibacterial Activity of New 6''-Modified Tobramycin Derivatives, *Antibiotics*, **13**, 1191, doi: https://doi.org/10.3390/antibiotics13121191.
15. Wang, M., Carver, J. J., Phelan, V. V., Sanchez, L. M., Garg, N., Peng, Y., Nguyen, D. D., Watrous, J., Kapono, C. A., Luzzatto-Knaan, T., Porto, C., Bouslimani, A., Melnik, A. V., Meehan, M. J., Liu, W. T., Crusemann, M., Boudreau, P. D., Esquenazi, E., Sandoval-Calderon, M., Kersten, R. D., et al. (2016) Sharing and community curation of mass spectrometry data with Global Natural Products Social Molecular Networking, *Nature biotechnology*, **34**, 828–837, doi: https://doi.org/10.1038/nbt.3597.
16. Nakamura, Y., Gojobori, T., and Ikemura, T. (2000) Codon usage tabulated from international DNA sequence databases: status for the year 2000, *Nucleic acids research*, **28**, 292, doi: https://doi.org/10.1093/nar/28.1.292.
17. Rudorf, S., and Lipowsky, R. (2015) Protein Synthesis in *E. coli*: Dependence of Codon-Specific Elongation on tRNA Concentration and Codon Usage, *PloS one*, **10**, e0134994, doi: https://doi.org/10.1371/journal.pone.0134994.
18. Sharp, P. M., and Li, W. H. (1987) The codon Adaptation Index--a measure of directional synonymous codon usage bias, and its potential applications, *Nucleic acids research*, **15**, 1281–1295, doi: https://doi.org/10.1093/nar/15.3.1281.
19. Zaytsev, K., Bogatyreva, N., and Fedorov, A. (2024) Link Between Individual Codon Frequencies and Protein Expression: Going Beyond Codon Adaptation Index, *International journal of molecular sciences*, **25**, 11622, doi: https://doi.org/10.3390/ijms252111622.
20. Cappannini, A., Ray, A., Purta, E., Mukherjee, S., Boccaletto, P., Moafinejad, S. N., Lechner, A., Barchet, C., Klaholz, B. P., Stefaniak, F., and Bujnicki, J. M. (2024) MODOMICS: a database of RNA

modifications and related information. 2023 update, *Nucleic acids research*, **52**, D239–244, doi: https://doi.org/10.1093/nar/gkad1083.

21. Rocha, E. P. (2004) Codon usage bias from tRNA's point of view: redundancy, specialization, and efficient decoding for translation optimization, *Genome research*, **14**, 2279–2286, doi: https://doi.org/10.1101/gr.2896904.